Technical Report

Development of High-Strength Low-Alloy Steel for High-Pressure Hydrogen Gas Accumulator

Misaho YAMAMURA* Tomohiko OMURA
Eisuke NAKAYAMA

Abstract

Reducing the cost of installing hydrogen stations is required in order to realize a hydrogen society. One way to reduce the cost of high-pressure hydrogen accumulators used in hydrogen stations is to reduce the number of hydrogen accumulators installed per location by increasing the capacity of the accumulators. On the other hand, considering the hardenability and manufacturability of steel materials, high-strength low-alloy steel with thin-wall design is required to achieve larger capacity. In order to find high-strength and hydrogen-compatible steels, hydrogen compatibility and accumulator compatibility were evaluated for Mo-V added steels and JIS standard steels for existing accumulator steels as a comparison. The results of this study are as follows.

1. Introduction

In combination with renewable energy, hydrogen is expected to play a part in the energy system which realizes CO_2-free. In the meantime, under the current hydrogen utilization situation, the popularization of fuel-cell vehicles and the development of hydrogen stations which supply hydrogen to fuel-cell vehicles constitute the core in the dissemination of hydrogen. As of 2023, there are 167 hydrogen stations in Japan. Towards further dissemination in future, reduction of the building cost of hydrogen stations is necessary, and even for individual equipment, cost reduction is required as well.

In hydrogen stations, accumulators bear the role of temporarily storing hydrogen gas of a maximum of 82 MPa, and are therefore required to have excellent pressure resistance performance and safety for use in the hydrogen environment. Accordingly, the low-alloy steels used for steel accumulators need to be equipped with high-strength and hydrogen embrittlement resistance properties compatibly.

Reduction of the number of installations of accumulators per station by enlarging the capacity of accumulators is one of the methods to reduce the cost of accumulators. On the other hand, the thickness in design is increased in order to secure pressure resistance performance. In order to realize cost reduction by enlarging the capacity taking into account the hardenability of low-alloy steels and the manufacturing capability of existing production facilities, it is estimated that steels having a tensile strength of 1 000 MPa or above usable under a high-pressure hydrogen environment, and thereby realizing wall thinning are required.[1] However, as the strength of low-alloy steels increases, deterioration of their properties due to hydrogen becomes remarkable.[2–4] For this reason, existing JIS standard steels SCM435 and SNCM439, which are generally used for accumulators, are used with a reduced tensile strength of 900 MPa or below to ensure hydrogen embrittlement resistance properties (hydrogen compatibility).

As for the hydrogen embrittlement resistance properties of low-alloy steels, it is widely known that low-alloy steels added with Mo and V (hereafter referred to as Mo-V-added steels) exhibit excellent hydrogen embrittlement resistance properties in the fields of oil well pipes and high tension strength bolts.[5–7] The mechanism by which Mo-V-added steels have excellent hydrogen embrittlement resistance properties is considered to be the hydrogen trapping effect of fine Mo-V carbides,[8, 9] the effect of reducing dislocation density due to high temperature tempering realized by high temper softening resistance,[10] and the effect of suppressing the grain boundary fracture by suppressing and spheroidizing the grain boundary carbides.[7] In addition, it has been clarified that Mo-V-added steels have higher properties[11] under the hydrogen gas environment at 45 MPa, when compared in terms of hydrogen embrittlement resistance properties with existing SCM435 steel having the same strength. However, the use of Mo-V-added steels at normal operation pressure of 70 MPa class hydrogen stations (maximum 82 MPa) has not been studied,

* Researcher, Applied Mechanics Laboratory, Materials Reliability Research Lab., Steel Research Laboratories
1-8 Fuso-cho, Amagasaki City, Hyogo Pref. 660-0891

and the effect of chemical compositions on hardenability and hydrogen embrittlement resistance properties have not been investigated either. Furthermore, toward the application to accumulators, it is necessary to judge the acceptability of design based on the evaluation of the life of accumulators based on trial design (hereafter referred to as trial design evaluation).

In this study for Mo-V added steels, by varying alloying elements, we evaluated hardenability, and then the hydrogen compatibility conforming to the Technical Document for safety use of the Compressed Hydrogen Facility (Accumulator and Compressor) made of low alloy steels used in the Hydrogen Refueling Station JPEC-TD0003 (hereafter referred to as the Low-alloy Steel Technical Document)[12]. In addition, the steel with good properties was subjected to fatigue crack growth analysis conforming to the "Standard for superhigh-pressure gas equipment KHKS 0220 (hereafter referred to as KHKS 0220)[13]", and based on the analysis, we conducted trial design evaluation, and judged the acceptability of the design of a large capacity accumulator to which Mo-V added steel has been applied.

Furthermore, this research and development was performed as part of the study on the application of high-strength low-alloy steel to reduce the cost of high-pressure hydrogen accumulators under the project "Development of Technologies for Hydrogen Refueling stations" of the New Energy and Industrial Development Organization (NEDO).

2. Experimental Method

2.1 Sample material

Chemical compositions of sample materials are shown in **Table 1**. The Mo-V-added steels in Table 1 are based on Mo-0.10V steel or SNB16 steel of JIS G 4107, and the alloy contents were varied in the ranges of 0.09–0.38%V, 0.50–1.27%Cr, and 0.66–1.55%Mo. Furthermore, B (boron)[14, 15] was added to the 0.5Cr-1.3Mo-B steel which is expected to improve hardenability. The chemical compositions of the comparison steels were those of the existing SCM435 and SNCM439 steels used for accumulators. These steels were vacuum-smelted on the laboratory base process, and hot-forged to round bars and plate materials, respectively. Round bars were subjected to soaking heat treatment, and 25 mmΦ × 100 mm test specimens were taken for hardenability evaluation. The plate materials were hot-rolled to a thickness of 12 mm and 35 mm, heated to 920°C for Mo-V-added steels, and to 900°C for the comparison steels, and then water-quenched. The strength was varied by changing the tempering temperature conditions at 1 to 4 levels, and round bar tensile test specimens for hydrogen compatibility evaluation were taken from the 12 mm thick plate, and 1T-CT test specimens for trial design evaluation were taken from the 35 mm thick plate. In Table 1, the critical cooling rate $V_{C\text{-}90}$ (°C/s) with which 90% martensitic structure can be obtained[16] is taken as the index of hardenability predicted from alloy compositions, and the values calculated from Formula (1) or (2), and the items of experiments performed for each steel grade are shown together.

B-added steel $V_{C\text{-}90}$ (°C/s)

$$= \exp\{2.94 - 0.75(2.7C + 0.4Si + Mn + 0.45Ni + 0.8Cr + 2.0Mo)\} \quad (1)$$

B-free steel $V_{C\text{-}90}$ (°C/s)

$$= \exp\{2.94 - 0.75(2.7C + 0.4Si + Mn + 0.45Ni + 0.8Cr + Mo) - 1\} \quad (2)$$

2.2 Hardenability evaluation

The Jominy test was performed to evaluate hardenability. The test specimens were held in an Ar atmosphere heating furnace at 920°C for the Mo-V-added steels, and at 900°C for the comparison steels, and then quenched at one end by cooling the test specimens from one side with a jet of water. After quenching, the side of the test specimen was machined in parallel to the longitudinal direction to a depth of approximately 1.6 mm, and polished in parallel to a finish. Rockwell hardness was measured at a specified interval on the polished surface from the hardened end face of the test specimen, and hardenability was evaluated by the hardness change from the hardened end face.

2.3 Hydrogen compatibility evaluation

To evaluate hydrogen compatibility, slow strain rate tests (SSRT) were performed at a strain rate of 3.0×10^{-6}/s in air at room temperature, and in high-pressure hydrogen gas at 85 MPa. **Figure 1** shows the schematic diagram of the stress-displacement diagram for determining hydrogen compatibility described in the Low-alloy Steel Technical Document[12]. In Fig. 1 (a), hydrogen compatibility is determined as existing when the displacement value of the maximum stress in the stress-displacement diagram in hydrogen exceeds the displacement value of the maximum stress shown in the stress-dis-

Table 1 Chemical compositions

(mass%)

	Material	C	Si	Mn	Cr	Mo	V	Nb	Other	$V_{C\text{-}90}$ (°C/s)	Experiment
Mo-V added steels	Mo-0.10V	0.40	0.19	0.44	1.25	0.73	0.10	0.025	–	3.27	SSRT
	Mo-0.26V	0.40	0.20	0.45	1.27	0.76	0.26	0.025	–	3.16	Jominy, SSRT
	SNB16	0.38	0.19	0.61	1.05	0.66	0.26	0.026	–	3.60	Jominy, SSRT, K_{IH}
	1.5Mo	0.36	0.20	0.62	1.05	1.55	0.38	0.026	–	1.90	Jominy, SSRT
	0.5Cr	0.39	0.20	0.63	0.51	0.67	0.37	0.026	–	4.76	Jominy, SSRT
	0.5Cr-1.5Mo	0.38	0.20	0.58	0.50	1.49	0.36	0.024	–	2.74	Jominy, SSRT
	SNB16-B	0.32	0.19	0.65	1.02	0.66	0.09	0.027	Ti: 0.026, B: 0.0015 N: 0.0040	1.11	Jominy
	0.5Cr-1.3Mo-B	0.30	0.19	0.63	0.52	1.32	0.09	0.025	Ti: 0.026, B: 0.0012 N: 0.0041	0.57	Jominy, SSRT, K_{IH}, FCGR*
Comparison steel	SCM435	0.38	0.20	0.61	0.92	0.30	–		–	5.08	Jominy, SSRT
	SNCM439	0.37	0.21	0.62	0.92	0.30			Ni: 2.0 O: 0.001	2.62	Jominy, SSRT, K_{IH}, FCGR*

* Fatigue crack growth rate, FCGR

placement diagram in air, and the maximum value is shown in hydrogen as well as in air. On the other hand, if the maximum value is not shown as in Fig. 1 (b), it is judged as incompatible with hydrogen. SSRT was performed on each of the steels having varied strengths, and the critical tensile strength which indicates hydrogen compatibility (hereafter referred to as critical tensile strength) was evaluated.

2.4 Trial design evaluation

Fatigue crack growth analysis was conducted for the trial design evaluation. **Figure 2** shows a schematic diagram of fatigue crack growth analysis. In the fatigue crack growth analysis, assuming the load variations in actual accumulators, the critical crack length is evaluated by the fracture toughness properties under the hydrogen environment (stress intensity factor at the lower threshold of hydrogen-assisted cracking, K_{IH}), the number of cycles to reach the critical crack length is evaluated by the fatigue crack growth properties under the hydrogen environment respectively, and the value with the safety margin taken into consideration is adopted as the permissible number of cycles.

Fatigue crack growth tests were performed conforming to KHKS 0220[13] and ASTM E647[17] at room temperature in 90 MPa high-pressure hydrogen gas under the conditions of a stress ratio of 0.1, and the constant controlled load (ΔP) of a sinusoidal wave provided at a frequency of 1 Hz.

The rising load tests for the evaluation of K_{IH} were performed conforming to KHKS 0220[13] at room temperature in air and in 90 MPa high-pressure hydrogen gas, controlling the aperture displacement rate to 0.0002 mm/s by displacement control (stress intensity factor rate dK/dt = 0.06 MPa·m$^{1/2}$/s). The load-displacement diagrams in air and hydrogen are superimposed, and the point at which the load-displacement diagram in hydrogen deviates from the load-displacement diagram in air under the same load is defined as the hydrogen-induced crack growth initiation point. K_{IH} was sought based on ASTM E399[18] from the crack lengths measured by forced fracture of the test specimens after the test.

As preconditions for fatigue crack growth analysis, it was assumed that the inner surface of the cylindrical body was subjected to repetitive stress loads of 82 MPa and 50 MPa in a 450 L accumulator, whose capacity is 1.5 times larger than that of a 300 L accumulator which is the mainstream accumulator in Japan. The initial flaw was assumed to be a semi-ellipsoidal shape in the axial direction having a surface length of 1.60 mm and a depth of 0.53 mm, and this time, the design was judged as valid when 1/4 of the critical crack depth based on the hydrogen environment characteristics obtained from tests is greater than the initial crack depth.

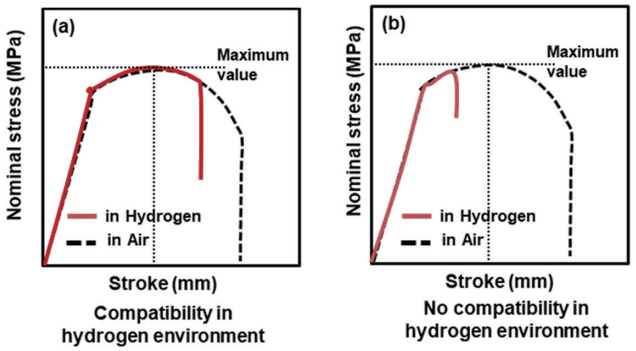

Fig. 1 Schematic diagram for determining hydrogen compatibility based on nominal stress-stroke diagrams for SSRT in air and hydrogen environments (a) compatibility in hydrogen environment, (b) no compatibility in hydrogen environment

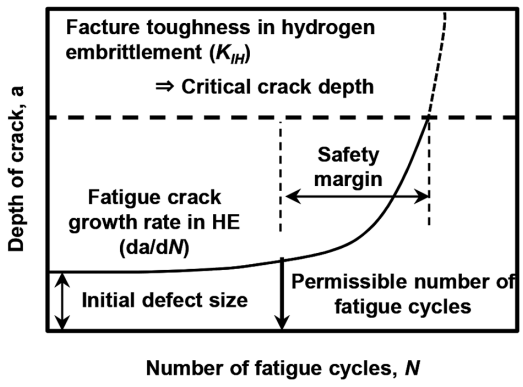

Fig. 2 Schematic diagram of fatigue crack growth analysis

3. Result

3.1 Result of hardenability evaluation

Figure 3 shows the relationship between $V_{C\text{-}90}$ predicted from the alloy compositions in Table 1 (hereafter referred to as calculated values) and $V_{C\text{-}90}$ obtained experimentally from the Jominy test (hereafter referred to as observed values). Herein, the observed value is obtained from the Jominy distance[19] at which the martensitic structure is considered to be 90%[20] based on the martensitic ratio estimated from the carbon content and Rockwell hardness. Among the Mo-V-added steels, the calculated and observed values of $V_{C\text{-}90}$ of the Mo-0.26V steel with 0.66–0.76%Mo, SNB16 steel, and 0.5Cr steel exhibit good agreement. On the other hand, regarding the 1.5%Mo steel, 0.5Cr-1.5Mo steel, 0.5Cr-1.3Mo-B steel, and SNB16-B steel, the observed values of $V_{C\text{-}90}$ are larger than the calculated values, suggesting that the actual hardenability is inferior to the calculated values. As for the comparison materials, the observed values of $V_{C\text{-}90}$ are smaller than the calculated values, suggesting that the actual hardenability is superior to those of the calculated values. This is considered to be attributed to the smaller crystal grain size number of the comparative steels evaluated in this study. Comparing the hardenability of the different steel grades using the observed $V_{C\text{-}90}$ values, the SNCM439 steel has the lowest $V_{C\text{-}90}$ value, indicating that it has excellent hardenability. Furthermore, comparing Mo-V-added steels and SCM435 steel, $V_{C\text{-}90}$ of Mo-0.26V with 1.05 to 1.27%Cr, SNB16 steel, and 1.5Mo steel are approximately equal to

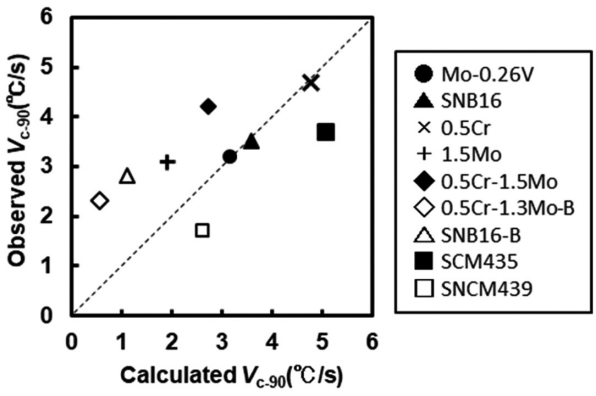

Fig. 3 Relationship between observed and calculated values of $V_{C\text{-}90}$

that of SCM435 steel, indicating that they have equal hardenability. 0.5%Cr steel and 0.5Cr-1.5Mo steel with 0.5%Cr have higher $V_{C\text{-}90}$, and have hardenability inferior to SCM435 steel. 0.5Cr-1.3Mo-B steel and SNB16-B steel with B addition have $V_{C\text{-}90}$ lower than that of SCM435 steel, suggesting that they have excellent hardenability. **Figure 4** shows the relationship between the observed $V_{C\text{-}90}$ and alloy content to clarify the effect of chemical compositions on the hardenability of Mo-V-added steels. With the increase in Cr, Mo, and B content, the $V_{C\text{-}90}$ value decreases, thereby enhancing the hardenability. Furthermore, a comparison between the calculated values and experimental measurements of the changes in $V_{C\text{-}90}$ due to the increased alloy content, from Fig. 4(a) for Cr, the changes of the calculated values and the observed values of $V_{C\text{-}90}$ are in agreement with each other, and it is confirmed that an effect of improving hardenability similar to that of the conventional findings[16] has been obtained. In the meantime, from Figs. 4(b) and (c), for Mo and B, the decrease in $V_{C\text{-}90}$ with increasing alloy content is smaller in the observed values than in the calculated values, and it has been clarified that the hardenability improving effect is smaller than that of the conventional finding[16]. The mechanism of Mo and B acting on hardenability will be studied later.

3.2 Result of hydrogen compatibility evaluation

Figure 5 shows the critical tensile strength of Mo-V-added steels and the comparison steels. Comparing the critical tensile strength among the steels, 0.5Cr-1.5Mo steel exhibits the highest critical tensile strength, and is considered to have excellent hydrogen embrittlement resistance properties. Furthermore, the critical tensile strength of Mo-V-added steels is higher than that of SCM435 steel, and the trend of superiority in hydrogen embrittlement resistance properties is consistent with the conventional findings.[11] In Mo-V-added steels, only the 0.5Cr steel does not achieve the target performance of the critical tensile strength of 1 000 MPa or above. On the other hand, as for the steels for comparison, SNCM439 steel achieves the target performance. This result suggests that the hydrogen embrittlement resistance properties of SNCM439 steel evaluated in this study are higher than those of the SNCM439 steel known from conventional findings[2]. The reason for this is that the sample material prepared by laboratory smelting, as compared with the material bought from market and evaluated, and as clarified by the past research pertaining to the application of SNCM439 steel to accumulators,[21] has higher hydrogen embrittlement resistance properties due to the lower O content and fewer oxide inclusions that cause fracture. Furthermore, although the critical tensile strength of the 0.5Cr-1.3Mo-B steel has not been confirmed, the tensile strength (TS) used in the evaluation of the trial design described below is 1 175 MPa, and conformity to hydrogen-compatibility is indicated and confirmed. **Figure 6** shows the relationship between the critical tensile strength and the alloy content to clarify the effect of chemical compositions on the critical tensile strength of Mo-V-added steels. Figure 6(a) shows that Cr exhibits a different trend depending on the Mo content. With 0.65%Mo, the critical tensile strength increases along with the increase of the Cr content, and with 1.5%Mo, it decreases. Figure 6(b) shows that the critical tensile strength increases with the increase of the Mo content for both 0.5%Cr and 1.0%Cr, and this trend is particularly remarkable for 0.5%Cr. As for V, Fig. 6(c) shows that the critical tensile strength decreases with the increase of the V content.

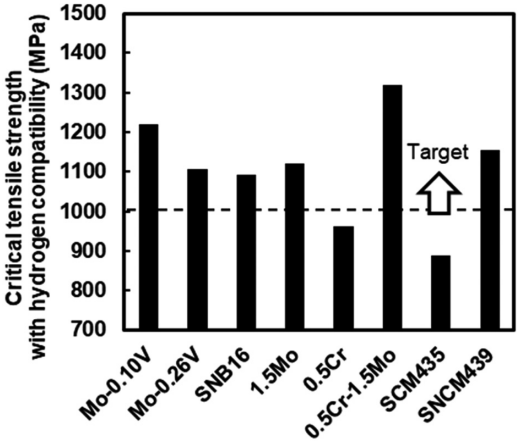

Fig. 5 Critical tensile strength with hydrogen compatibility of Mo-V added steels and comparison steels

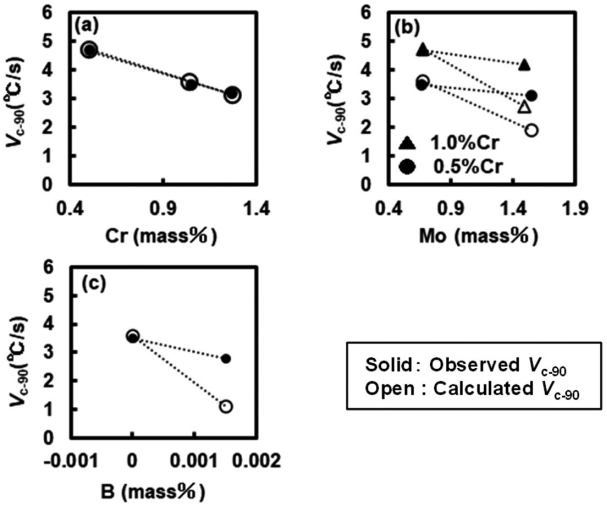

Fig. 4 Relationship between $V_{C\text{-}90}$ and alloy content of (a) Cr, (b) Mo and (c) B

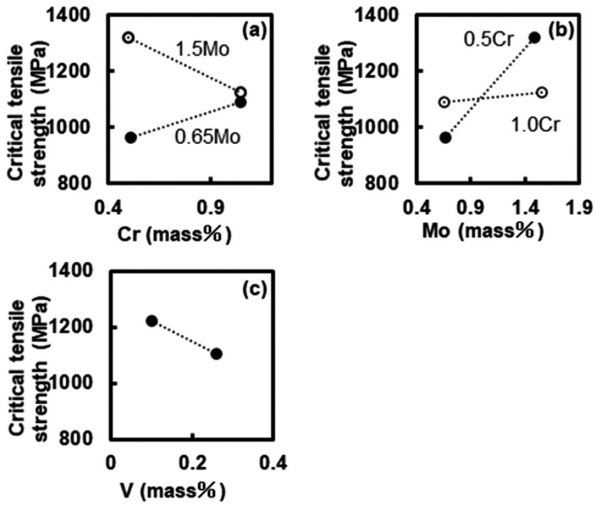

Fig. 6 Relationship between critical tensile strength and alloy content of (a) Cr, (b) Mo and (c) V

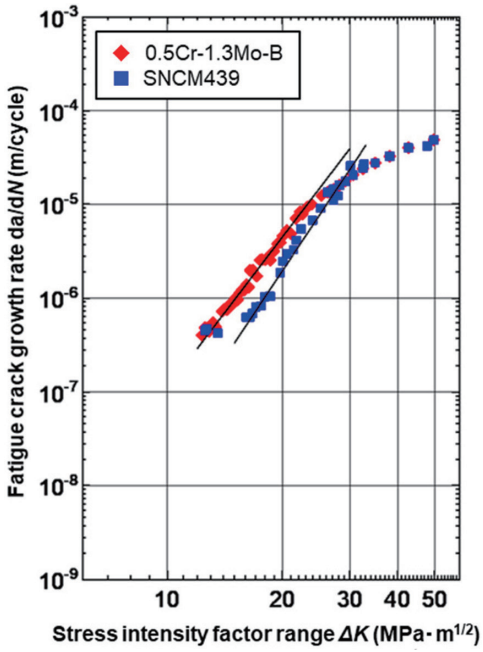

Fig. 7 Fatigue crack growth rate, da/d*N*, versus stress intensity factor range, *ΔK*, for 0.5Cr-1.3Mo-B and SNCM439

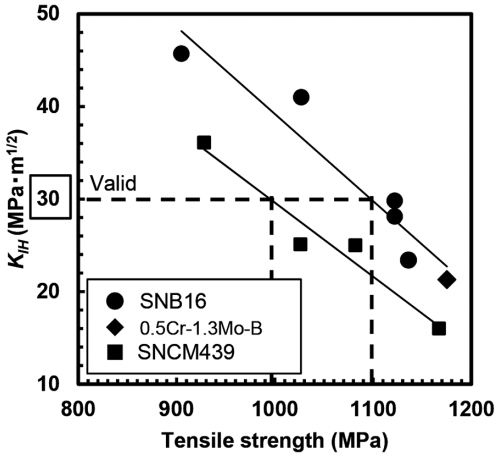

Fig. 8 Relationship between K_{IH} and tensile strength of SNB16, 0.5Cr-1.3Mo-B and SNCM439

3.3 Result of trial design evaluation

Figure 7 shows the relationship between the fatigue crack growth rate and the stress intensity factor obtained from the fatigue crack growth tests of 0.5Cr-1.3Mo-B steel (TS: 1 175 MPa) and SNCM439 steel (TS: 1 026 MPa) at 90 MPa high pressure hydrogen gas at room temperature. The fatigue crack growth rate of 0.5Cr-1.3Mo-B steel under the hydrogen environment is higher than that of SNCM439 steel, the phenomenon of which is considered to be due to the difference in strength properties. The fatigue crack growth rate analysis was conducted in accordance with KHKS 0220[13], and from the fatigue crack growth rate under the hydrogen environment, conditions under which 1/4 of the critical crack depth becomes larger than the initial crack depth were calculated. The design is valid for $K_{IH} \geq 30$ MPa·m$^{1/2}$ for all steel grades.

Figure 8 shows the relationship between K_{IH} and the tensile strength of the sample materials obtained from the rising load test. As strength-varied SNB16 steels and the 0.5Cr-1.3Mo-B steel (TS: 1 175 MPa) are compared, regardless of the difference in chemical compositions, K_{IH} and tensile strength of the Mo-V-added steels are in a proportionality relation, and K_{IH} tends to decrease in line with the increase of tensile strength. Furthermore, when the Mo-V added steels and the strength-varied SNCM439 steels are compared, Mo-V-added steels exhibit strength-toughness balance superior to that of SNCM439 steels. The relationship between the tensile strength and K_{IH} of SNCM439 steel smelted on the laboratory base is generally consistent with the trend found in the conventional findings[22].

The tensile strength calculated from the fatigue crack growth analysis which satisfies $K_{IH} \geq 30$ MPa·m$^{1/2}$ as a condition for validating design is about 1 100 MPa for the Mo-V added steels, and about 1 000 MPa for the SNCM439 steel, respectively, and it was confirmed that the design is valid at the strength above the target performance in both steels.

4. Study

4.1 Influence of alloying metal on hardenability

Regarding the influence of Mo and B on hardenability, Fig. 3 suggests that the actual hardenability of steel grades added with 1.5mass% Mo and B is inferior to those predicted from the alloy compositions. Furthermore, from Figs. 4 (b), (c), it has been clarified that the effect of increasing the contents of Mo and B on hardenability is smaller than the effect suggested by conventional findings. As a reason, this is considered to be due to the influence of C and Mo partly becoming undissolved carbides during quenching. Inoue et al.[23] calculated the contents of dissolved C and Mo effective for improving hardenability (hereafter referred to as effective contents of C and Mo) based on the quantitative analysis of the contents of undissolved carbides in steel with 0.3–0.6%C and 0–2.0%Mo, and redetermined the hardenability, and clarified that the actual observed values and calculated values agree well. The contents of effective C and Mo for 1.5Mo steel and 0.5Cr-1.5Mo steel were sought by using the method proposed by Inoue et al.[24] to predict the content of undissolved carbides, and in **Table 2**, the result of redetermining the observed $V_{C\text{-}90}$ from the calculated $V_{C\text{-}90}$ value and the content of effective C is shown. The recalculated values of $V_{C\text{-}90}$ obtained with the effective contents of C and Mo nearly agree with the observed values, and for the aforementioned steel with the addition of 1.5mass% Mo, the effect of hardenability improvement is considered to be smaller than that of the conventional findings[16] due to the influence of undissolved carbides. Furthermore, as for B for the improvement of hardenability, it is assumed that the existence of dis-

Table 2 Comparison of added and effective C and Mo content of $V_{C\text{-}90}$

Material	Added C	Added Mo	Calculated $V_{C\text{-}90}$ (°C/s)	Observed $V_{C\text{-}90}$ (°C/s)	Effective C	Effective Mo	Calculated $V_{C\text{-}90}$ (°C/s)	Observed $V_{C\text{-}90}$ (°C/s)
1.5Mo	0.36	1.55	1.90	3.1	0.34	1.00	3.0	2.9
0.5Cr-1.5Mo	0.38	1.49	2.74	4.2	0.36	1.08	3.9	3.9

solved B of 5 ppm or more at the grain boundary is required.[25] The content of dissolved B in SNB16-B steel was estimated from B, Ti, and N,[26] and calculated to be 0.0015% (15 ppm). Therefore, it is considered that the content of dissolved B is sufficient to improve hardenability. However, the effect of B on hardenability improvement is affected by interactions with other elements[25] and/or quenching conditions[27]. In order to maximize the effect of B addition, it is necessary to clarify these effects in Mo-V-added steels.

Hardenability and the alloy design required to enlarge the capacity of accumulators are described. First of all, it is difficult to determine unconditionally the threshold value of hardenability required for steel materials because hardenability depends on the cooling capacity determined by the equipment used to manufacture the accumulators and the refrigerant liquid to be used. On the other hand, assuming that large-capacity accumulators are manufactured utilizing existing facilities, it is desirable that the hardenability be equivalent to or above that of existing steels. Figure 3 shows that, when compared with SCM435 steel, hardenability of the Mo-V-added steels is similar to or higher than that of the SCM435 steel, except for the 0.5Cr and 0.5Cr-1.5Mo steels. In particular, since the hardenability of 0.5Cr-1.3Mo-B steel and SNB16-B steel with the addition of B is excellent, improvement of hardenability by utilizing B is considered desirable in alloy design.

4.2 Effect of alloying element on hydrogen embrittlement resistance properties

Concerning the influence of Cr on critical tensile strength, Fig. 6 shows that the critical tensile strength of 1.5%Mo decreases with the increase of the Cr content, while that of 0.65%Mo increases contrarily. The cause of the deterioration of hydrogen embrittlement resistance properties of 1.5%Mo along with the increase of the Cr content is considered to be the present state of the carbides precipitated on the former γ grain boundary. Suppression of carbides M_3C and $M_{23}C_6$ formed at the former γ grain boundary has the effect of preventing the grain boundary fracture type hydrogen embrittlement.[28] Furthermore, M_3C and $M_{23}C_6$ increase with increased addition of Cr and Mo. Therefore, it is considered that, for 1.5%Mo steel, the formation of harmful boundary carbides is suppressed along with the decrease of the Cr content, and that, therefore, hydrogen embrittlement resistance properties are improved. On the other hand, for 0.65%Mo steel, there are other microstructural factors considered to be affecting the hydrogen embrittlement resistance properties; however, this has not been clarified in this study.

As for the effect of Mo on critical tensile strength, Fig. 6(b) shows that in both cases of 1.0%Cr and 0.5%Cr, the hydrogen embrittlement resistance properties become higher with the increase in Mo content, and this trend is especially significant in 0.5%Cr. The improvement of hydrogen embrittlement resistance properties along with the increase of the Mo content shows the same trend as the one shown in the conventional findings.[29–31] As reasons for Mo improving hydrogen embrittlement resistance properties, the following effects are considered: suppression of grain boundary fracture by the spheroidized cementite realized by high tempering temperature,[32] increase in critical hydrogen concentration leading to fracture due to hydrogen trapping by Mo_2C,[29, 30] and the grain boundary fracture being suppressed due to bonding strength on the former γ grain boundary increased by Mo[5]. This time as well, it is considered that the same mechanism has worked, and Mo addition has improved the hydrogen embrittlement resistance properties.

As for the effect of V on critical tensile strength, Fig. 6(c) shows that the hydrogen embrittlement resistance properties deteriorate as the content of V increases from 0.10% to 0.26%. However, many conventional findings indicated that the hydrogen embrittlement resistance properties are improved by increasing V addition,[33–35] and the present result is different from the conventional findings. On the other hand, Seo et al.[36] suggested that V tends to retain undissolved carbides during quenching, and coarsens them during tempering, becoming fracture initiation points in a hydrogen environment, thereby deteriorating hydrogen embrittlement resistance properties. In this study, since the alloy compositions had relatively high contents of V and Mo which tends to retain undissolved carbides, the hydrogen embrittlement resistance properties are considered to deteriorate by the same mechanism as that of the V content that increased from 0.10%V to 0.26%V. Furthermore, when considering SCM435 steel as a material without V addition and comparing it with a material with 0.10%V, it can be concluded that the addition of 0.10%V significantly enhances the hydrogen embrittlement resistance properties.

4.3 Alloy metal design of low-alloy steel for high-pressure hydrogen accumulator

In Sections 4.1 and 4.2, the effects of alloying elements on hardenability and hydrogen embrittlement resistance properties were studied. The alloy design incorporated with both properties required for accumulators is described. For hardenability, the addition of Cr and B is effective, and the addition of Mo is effective for hydrogen embrittlement resistance properties. However, it has been clarified that hardenability deteriorates when Mo forms undissolved carbides. Therefore, it is desirable to add the maximum amount of Mo that can be dissolved during quenching at the maximum heat treatment temperature of the quenching facility. Furthermore, since Cr is estimated to deteriorate the hydrogen embrittlement resistance properties when Mo is dissolved, it is recommended that the hardenability improvement by B addition be maximized, and then a minimum amount of Cr be added to compensate for the lack of hardenability. Furthermore, V is very effective in improving the hydrogen embrittlement resistance properties if it is dissolved during quenching; however, if undissolved carbides are formed, the hydrogen embrittlement resistance properties are considered to deteriorate. Therefore, similarly to Mo, it is desirable to add the maximum amount of V that can be dissolved during quenching. Since the 0.5Cr-1.3Mo-B steel prepared based on these alloys is confirmed to have hydrogen compatibility at a low temperature of −40°C at tensile strength 1 175 MPa and good hardenability, it was confirmed that this alloy design is effective for designing low-alloy steels for high-strength accumulators.

4.4 Evaluations of fracture toughness properties under hydrogen environment and trial design

The fatigue crack growth rate and the fracture toughness properties under the hydrogen environment of Mo-V-added steels were evaluated from Fig. 7 and Fig. 8, and it was confirmed from the fatigue crack growth analysis that the design with SNCM439 of about 1 000 MPa and Mo-V-added steels of about 1 100 MPa is valid, and the target performance of 1 000 MPa or above to realize cost reduction for enlarging capacity has been achieved. From this, it was concluded that Mo-V-added steels are particularly promising as the steel material for large-capacity high-pressure hydrogen accumulators.

As stated in the introduction, existing steels used for accumulators have reduced strength to ensure hydrogen compatibility. This is

considered to be based on the conventional findings that K_{IH} decreases with increasing strength, and that K_{IH} becomes equal for the same strength regardless of steel grade[37, 38]. However, as Fig. 8 shows, this research has clarified that the strength-toughness balance of Mo-V-added steel is superior to that of existing steel of SNCM439. Furthermore, it has been clarified that the same result is obtained when K_{IH} is evaluated by changing the stress intensity factor rate (dK/dt) in the range of 0.005 to 3 MPa·m$^{1/2}$/s.[39] Therefore, contrary to conventional findings, there is a clear difference in terms of K_{IH} between SNCM439 and Mo-V-added steels, depending on the type of steel. This is an achievement that proves that Mo-V-added steels can be applied to hydrogen environments with higher strength than that of conventional steels. However, we consider that it is necessary to expand the data to further prove the safety in the application of high-strength steels.

5. Conclusion

In order to realize cost reduction by increasing the capacity of high-pressure hydrogen accumulators, the effects of chemical compositions on hardenability and hydrogen embrittlement resistance properties, which are required for low-alloy steels, were investigated for Mo-V-added steels, and the alloy design guideline was clarified. Furthermore, from the result of the evaluation of the trial design based on the steel grades developed based on the obtained alloy design guideline, it was confirmed that the design is valid in terms of target performance. Thus we have concluded that Mo-V-added steels are promising as the steel material for large-capacity high-pressure hydrogen accumulators.

This article utilizes the results obtained in the “Development of Technologies for Hydrogen Refueling Stations” commissioned by the New Energy and Industrial Development Organization (NEDO).

References

1) New Energy and Industrial Development Organization (NEDO): Progress Report on: Development of Technoloies for Hydrogen Rufueling Staions / Development of technology related to cost for hydrogen refueling stations/Research and Development of New Type High-pressure Accumulator using High-strength Low-alloy Steel, 2023
2) Arashima, H. et al.: Tetsu-to-Hagané. 96 (2), 76 (2010)
3) Somerday, B.P. et al.: International Journal of Hydrogen Energy. 42, 7314 (2017)
4) Matsuoka, S. et al.: Transactions of the JSME (in Japanese). 83 (854), 1 (2017)
5) Matsumoto, H. et al.: Sumitomo Metals. 48 (4), 207 (1996)
6) Omura, T. et al.: Tetsu-to-Hagané. 91 (5), 478 (2005)
7) Omura, T. et al.: Materia Japan. 44 (1), 56 (2005)
8) Yamasaki, S. et al.: Tetsu-to-Hagané. 83 (7), 454 (1997)
9) Tsuchida, Y. et al.: Journal of High Pressure Institute of Japan. 52 (6), 323 (2014)
10) Kushida, T. et al.: Tetsu-to-Hagané. 82 (4), 297 (1996)
11) Omura, T. et al.: Zairyo-to-Kankyo. 63 (10), 528 (2014)
12) Japan Petroleum Energy Center (JPEC): Technical Document for safety use of Compressed Hydrogen Facility (Accumulator and Compressor) made of low alloy steels used in Hydrogen Refueling Station, JPEC-TD 0003, 2020
13) The High Pressure Gas Safety Institute of Japan: KHKS 0220, Standard for superhigh-pressure gas equipment, 2020
14) Llewellyn, D.T., Cook, W.T.: Metals Technology. 1 (12), 517 (1974)
15) Kapadia, B.M.: J. Heat Treat. 5 (1), 41 (1987)
16) Ueno, M., Itoh, K.: Tetsu-to-Hagané. 74 (6), 133 (1988)
17) ASTM E647-15^{e1}: Standard Test Method for Measurement of Fatigue Crack Growth Rates, 2015
18) ASTM E399-20: Standard Test Method for Linear-Elastic Plane-Strain Fracture Toughness of Metallic Materials, 2020
19) Ueno, M., Itoh, K.: Tetsu-to-Hagané. 74 (5), 166 (1988)
20) The Japan Institute of Metals and Materials (JIM), The Iron and Steel Institute of Japan (ISIJ): Iron and Steel Materials Handbook. Maruzen-Yushodo Company, Limited, 1967, p.87–89
21) New Energy and Industrial Development Organization (NEDO): Progress Report on: Research and Development Project for Hydrogen Utilization Technology/ Development for Rationalization of Domestic Regulations, Harmonization with International Standards and International Standardization for Fuel-cell Vehicle and Hydrogen Supply Infrastructure/ Development on Dissemination of Steel Material usable for Fuel-cell Vehicle and Related Equipment of Hydrogen Station, 2018
22) Arashima, H.: Study on embrittlement behavior of high-strength low-alloy steels in high-pressure hydrogen gas. Hokkaido University. Doctoral Theses, 2022
23) Inoue, T.: Tetsu-to-Hagané. 78 (2), 288 (1992)
24) Inoue, T.: Tetsu-to-Hagané. 78 (4), 616 (1992)
25) Ueno, M., Itoh, K.: Tetsu-to-Hagané. 74 (5), 910 (1988)
26) Lin, H., Cheng, G.: Materials Science and Technology. 3, 755 (1987)
27) Ishikawa, K. et al.: Tetsu-to-Hagané. 109 (1), 62 (2023)
28) Omura, T. et al.: Nippon Steel & Sumitomo Metal Technical Report. (107), 19 (2015)
29) Kushida, T., Kudo, T.: Zairyo-to-Kankyo. 41, 677 (1992)
30) Gojic, M., Kosec, L.: ISIJ International. 37 (4), 412 (1997)
31) Kimura, T., Nakamura, S.: DENKI-SEIKO. 65 (1), 31 (1994)
32) Omura, T.: Zairyo-Kankyo. 58, 138 (2009)
33) Ito, K.: Computational Materials Science. 218 (111951), 1 (2023)
34) Sakai, T. et al.: Tetsu-to-Hagané. 72 (9), 145 (1986)
35) Asahi, H. et al.: ISIJ International. 43 (4), 527 (2003)
36) Seo, H.J.: International Journal of Hydrogen Energy. 46, 19670 (2021)
37) Loginow, A.W., Phelps E.H.: Corrosion. 31 (11), 404 (1975)
38) Nibur, K.A.: Sandia Report. SAND2010-4633, Sandia National Laboratories, (2010)
39) Nakamura, Y. et al.: The 185th ISIJ Spring Meeting, Tokyo, March, 2023

Misaho YAMAMURA
Researcher
Applied Mechanics Laboratory
Materials Reliability Research Lab.
Steel Research Laboratories
1-8 Fuso-cho, Amagasaki City, Hyogo Pref. 660-0891

Tomohiko OMURA
Dr.Eng., Principal Researcher
Steel Research Laboratories

Eisuke NAKAYAMA
Dr.Eng., General Manager, Head of Laboratory
Applied Mechanics Laboratory
Materials Reliability Research Lab.
Steel Research Laboratories